International Journal of Thermophysics, Vol. 24, No. 1, January 2003 (© 2003)

Equations of State for Technical Applications. I. Simultaneously Optimized Functional Forms for Nonpolar and Polar Fluids

R. Span[1] and W. Wagner[2]

Received January 10, 2002

New functional forms for multiparameter equations of state have been developed for non- and weakly polar fluids and for polar fluids. The resulting functional forms, which were established with an optimization algorithm which considers data sets for different fluids simultaneously, are suitable as a basis for equations of state for a broad variety of fluids. With regard to the achieved accuracy, the functional forms were designed to fulfill typical demands of advanced technical application. They are numerically very stable, and their substance-specific coefficients can easily be fitted to restricted data sets. In this way, a fast extension of the group of fluids for which accurate empirical equations of state are available becomes possible. This article deals with characteristic features of the new class of simultaneously optimized equations of state. Shortcomings of existing multiparameter equations of state widely used in technical applications are briefly discussed, and demands on the new class of equations of state are formulated. Substance specific parameters and detailed comparisons are given in subsequent articles for the non- and weakly polar fluids (methane, ethane, propane, isobutane, *n*-butane, *n*-pentane, *n*-hexane, *n*-heptane, *n*-octane, argon, oxygen, nitrogen, ethylene, cyclohexane, and sulfur hexafluoride) and for the polar fluids (trichlorofluoromethane (CFC-11), dichlorodifluoromethane (CFC-12), chlorodifluoromethane (HCFC-22), difluoromethane (HFC-32), 1,1,2-trichlorotrifluoroethane (CFC-113), 2,2-dichloro-1,1,1-trifluoroethane (HCFC-123), pentafluoroethane (HFC-125),

[1] To whom correspondence should be addressed. Lehrstuhl für Thermodynamik und Energietechnik, Universität Paderborn, D-33095 Paderborn, Germany. E-mail: Roland.Span@thet.uni-paderborn.de

[2] Lehrstuhl für Thermodynamik, Ruhr-Universität Bochum, D-44780 Bochum, Germany. E-mail: Wagner@thermo.ruhr-uni-bochum.de

0195-928X/03/0100-0001/0 © 2003 Plenum Publishing Corporation

1,1,1,2-tetrafluoroethane (HFC-134a), 1,1,1-trifluoroethane (HFC-143a), 1,1-difluoroethane (HFC-152a), carbon dioxide, and ammonia) considered to date.

KEY WORDS: equation of state; extrapolation behavior; functional form; fundamental equation; Helmholtz energy; nonpolar fluids; numerical stability; polar fluids; simultaneous optimization; technical application.

1. INTRODUCTION

Over the course of the last two decades, the development of optimization algorithms has significantly increased the performance of empirical multiparameter equations of state. New generations of reference equations of state have become available both with a very high level of accuracy (see Refs. 1–6) which is required for scientific standards and for selected technical applications and with a level of accuracy which is required for typical technical standards (see, e.g., Refs. 7–12); for a comprehensive overview, see Ref. 13. Compared to older formulations, these equations of state are far superior with regard to the achieved accuracy, to their performance in the critical region, to their extrapolation behavior, and to their reliability for properties which are difficult to describe or for which no data were available when the equation was established. However, the development of a functional form is a time-consuming process which requires large and reliable data sets since it is numerically very flexible. Functional forms which are optimized on the basis of insufficient data sets may easily overturn the advantages of optimized equations of state. In addition, equations of state which were optimized for a specific fluid are less suitable for the description of different fluids, unless the fluids behave in a very similar way. Thus, equations of state with an optimized functional form are available only for a limited number of substances, and older equations of state without an optimized functional form are still in use in many technical applications where accurate thermodynamic property data are required for a broad variety of fluids.

This problem was addressed by Span et al. [14], who presented a new kind of optimization algorithm which considers data sets for different substances simultaneously. The chosen functional form is not the one which yields the best results for a certain fluid, but the one which yields on average the best results for all fluids. If the considered fluids are typical representatives of a certain group of fluids, such as the groups of nonpolar or polar fluids, equations of state using the simultaneously optimized functional form can be fitted to data sets for different fluids out of the same

group without significant disadvantages. In this way, the advantages of equations of state with an optimized functional form can be utilized for a multitude of fluids, even though the available data sets would not be sufficient to optimize a functional form using substance-specific algorithms in most cases.

As a first application, we used the simultaneous optimization algorithm to establish functional forms for equations of state which are able to satisfy advanced technical demands on accuracy for typical nonpolar and polar fluids but which are *not* intended as reference equations for well measured substances. This article gives the necessary background information on the development of this new class of equations of state. General aspects of the project are discussed in some detail, and the resulting functional forms are given. However, comparisons of the new equations of state with experimental data and with other equations of state remain on a very general level, and no substance-specific parameters are given here. To limit the size of this article, more detailed information is published in subsequent articles for the considered non- and weakly polar fluids (methane, ethane, propane, isobutane, *n*-butane, *n*-pentane, *n*-hexane, *n*-heptane, *n*-octane, argon, oxygen, nitrogen, ethylene, cyclohexane, and sulfur hexafluoride; see Ref. 15) and for the considered polar fluids (trichlorofluoromethane (CFC-11), dichlorodifluoromethane (CFC-12), chlorodifluoromethane (HCFC-22), difluoromethane (HFC-32), 1,1,2-trichlorotrifluoroethane (CFC-113), 2,2-dichloro-1,1,1-trifluoroethane (HCFC-123), pentafluoroethane (HFC-125), 1,1,1,2-tetrafluoroethane (HFC-134a), 1,1,1-trifluoroethane (HFC-143a), 1,1-difluoroethane (HFC-152a), carbon dioxide, and ammonia; see Ref. 16). Parameter sets for further fluids will follow.

2. THE STATUS QUO AND DEMANDS ON THE NEW CLASS OF MULTIPARAMETER EQUATIONS OF STATE

The multiparameter equations of state which are used in technical applications for a multitude of substances today (*technical equations of state* in contrast to highly accurate reference equations of state which are usually formulated in the Helmholtz energy) still belong to the group of so called *modified BWR equations*. In reduced form, this kind of pressure-explicit formulation can be written as

$$\frac{p}{\rho RT} = \sum_{i=1}^{I_{\mathrm{Pol}}} n_i \, \tau^{t_i} \, \delta^{d_i} + \sum_{i=I_{\mathrm{Pol}}+1}^{I_{\mathrm{Pol}}+I_{\mathrm{Exp}}} n_i \, \tau^{t_i} \, \delta^{d_i} \exp\left(-\gamma \, \delta^2\right) \tag{1}$$

where τ is the inverse reduced temperature T_r/T, δ the reduced density ρ/ρ_r, and R the gas constant.[3] The functional form of these equations (the values of I_{Pol}, I_{Exp}, t_i, and d_i) has not been optimized, but has been determined in a trial and error procedure. The coefficients n_i are substance-specific, and γ is usually chosen in a way such that $\gamma \simeq \rho_r^2/\rho_c^2$. For technical equations of state, the number of terms in Eq. (1) ranges from $I_{Pol}+I_{Exp}=8$ for the original BWR equation [17] to $I_{Pol}+I_{Exp}=19$ for the Bender equation [18] with several formulations in-between. Modified BWR equations of state with more terms have been used as reference equations of state (see, e.g., Ref. 19), but such formulations have only been established for well measured substances.

The performance of the original BWR equation and its simple modifications is hardly sufficient to satisfy current technical demands on the accuracy of thermodynamic property data. Figure 1 shows deviations between highly accurate experimental results for the density of carbon dioxide and values calculated from a typical cubic equation of state, the so called Trebble–Bishnoi–Salim (TBS) equation [23a], from an 8 term BWR equation and a 19 term Bender equation, which were fitted to the data set described in Ref. 16. The Bender equation describes the experimental results within $|\Delta\rho|/\rho \leqslant 0.2\%$ in general. Significantly larger deviations are observed in the extended critical region ($T_{c,CO2} = 304.1282$ K, $p_{c,CO2} = 7.3773$ MPa) and at far supercritical states. The original BWR equation yields typical deviations of the order of $|\Delta\rho|/\rho \approx 1$–$2\%$, but the limit of 2% is exceeded close to the saturated vapor line, in the extended critical region, and at high-pressure liquid states. The TBS equation of state describes the density of fluids with typical uncertainties of $|\Delta\rho|/\rho \approx 2$–$5\%$, and the limit of 5% is often exceeded in the extended critical region and at low temperature and/or high pressure liquid states.

Even larger deviations can be observed for caloric properties, especially for liquid states. Figure 2 shows deviations between reliable experimental results for the speed of sound in liquid *n*-butane and values calculated from Bender, BWR, and TBS equations of state. In general, Bender equations are able to represent derived caloric properties such as heat capacities or speeds of sound within about 1–2%. Larger deviations are usually observed in the extended critical region and for liquid states with low (reduced) temperature, as can be seen in Fig. 2. The original BWR equation and its simple modifications result in typical uncertainties of

[3] More often, modified BWR equations are given in dimensional form without reducing pressure, temperature, and density. The form given in Eq. (1) was chosen to underline the similarity with the equations presented in this article. For the necessary conversions see Ref. 13.

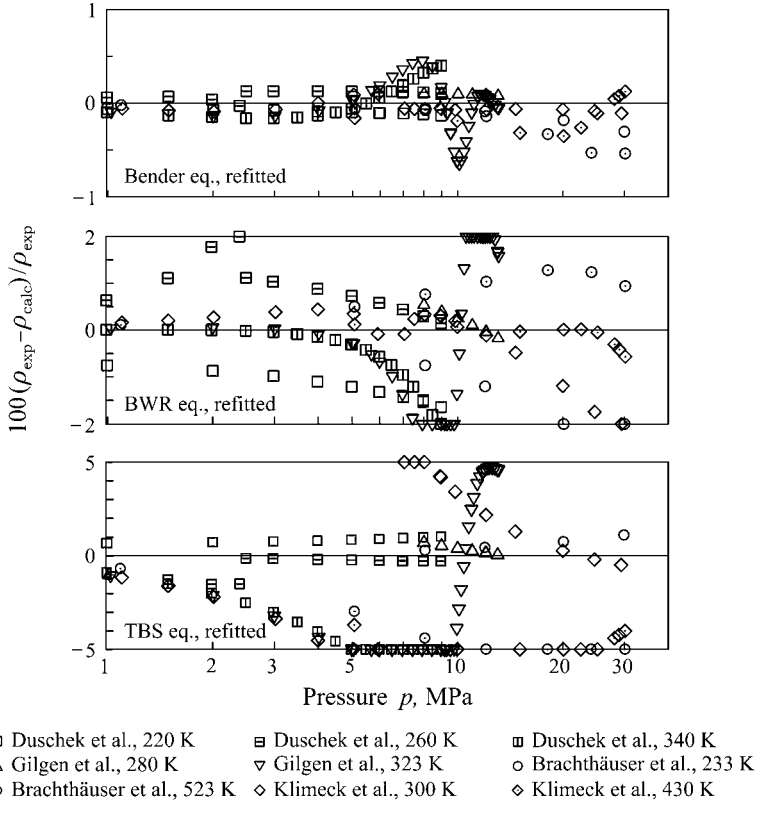

Fig. 1. Percentage deviations between experimental data for the density of carbon dioxide by Duschek et al. [20], Gilgen et al. [21], Brachthäuser et al. [22], and Klimeck et al. [23] and values calculated from refitted Bender, BWR, and TBS equations of state.

10–20% for liquid states and liquid-like supercritical states. The uncertainty of liquid phase speeds of sound calculated from typical cubic equations of state exceeds 50%.

While the observed uncertainties in density may still be acceptable for many technical applications, the uncertainties for derived caloric properties calculated from cubic equations of state or from the BWR equation and its simple modifications are unacceptable. Over a broad range of states, accurate and consistent data for thermal and caloric properties can only be calculated with rather complex modifications of the BWR equation.

However, more complex modified BWR equations also have serious disadvantages when being fitted to data sets of less well measured

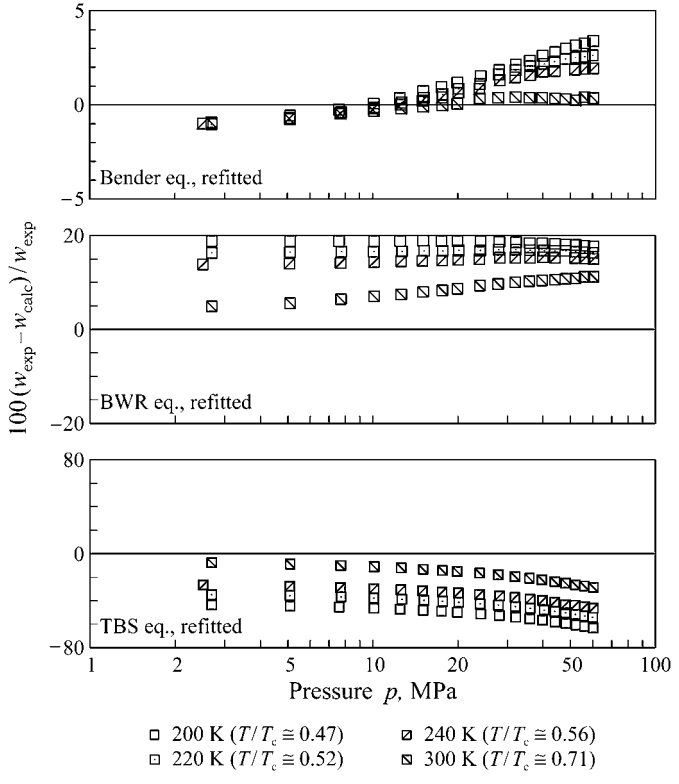

Fig. 2. Percentage deviations between experimental data for the speed of sound in the liquid phase of normal butane measured by Niepmann [24] and values calculated from refitted Bender, BWR, and TBS equations of state.

substances. In the range where experimental data are available, Bender equations yield reliable results for the properties used to fit the substance-specific coefficients. For *n*-octane, this fact is illustrated in the p-ρ diagram in Fig. 3. In the hatched area, where pvT data were used to fit the equations, a Bender equation fitted to the data set described in Ref. 15 and the Bender equation by Polt [25] yield similar and physically reasonable plots of the shown isotherms. Outside the range where the equations were fitted to data, both equations yield physically unreasonable results. For derived caloric properties, unreasonable results can be found even within the range where the equations were fitted to data. This fact is illustrated in the c_p-T diagram in Fig. 3.

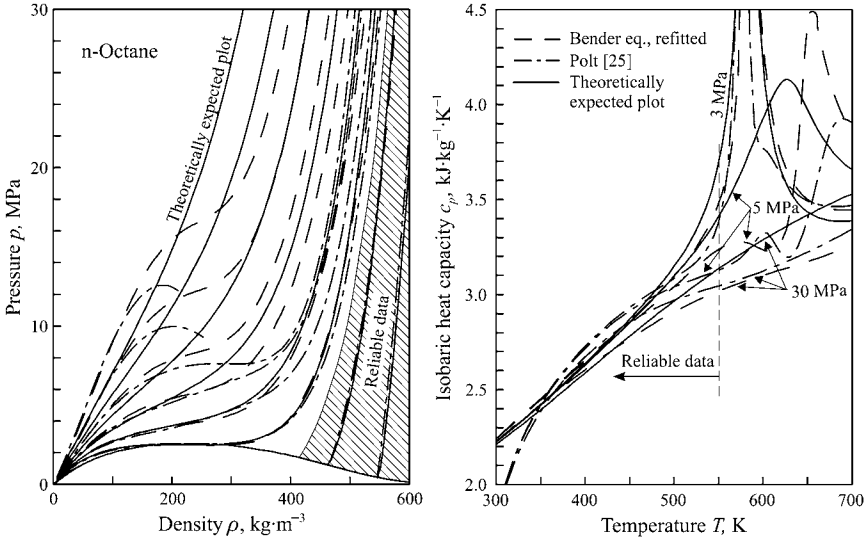

Fig. 3. Isotherms in a p-ρ diagram and isobars in a c_p-T diagram for *n*-octane which were calculated from the Bender equation published by Polt [25] and from a Bender equation which was refitted to the data set described in Ref. 15. The Maxwell-like loops which result from the equation by Polt at supercritical temperatures were cut to preserve the clarity of the p-ρ diagram.

The reason for this misbehavior becomes obvious in Fig. 4. The coefficients of complex multiparameter equations of state without an optimized functional form are highly intercorrelated. When being fitted to the small data sets available for higher alkanes, the equations are able to represent the data quite well, but the resulting coefficients are somewhat random. Such equations cannot be extrapolated to states outside the range where they were fitted to data, and calculated values for derived properties cannot be expected to be reasonable. The BWR equation and its simple modifications are numerically more stable, but especially with regard to an accurate description of caloric properties they fail due to their general restrictions.

Depending on the application, technical demands on the accuracy of thermodynamic property models can be very different. When dealing with mixtures of complex molecules, chemical engineers are grateful for a qualitatively correct description of the resulting phase equilibria, while engineers in the natural-gas business need to calculate densities of a multi-component mixture with an uncertainty of $|\Delta\rho|/\rho \leqslant 0.1\%$ up to pressures of 30 MPa. The equations of state presented here aim at technical applications with advanced, but not with extreme, demands on the accuracy of thermodynamic properties, which involve not only thermal properties but also

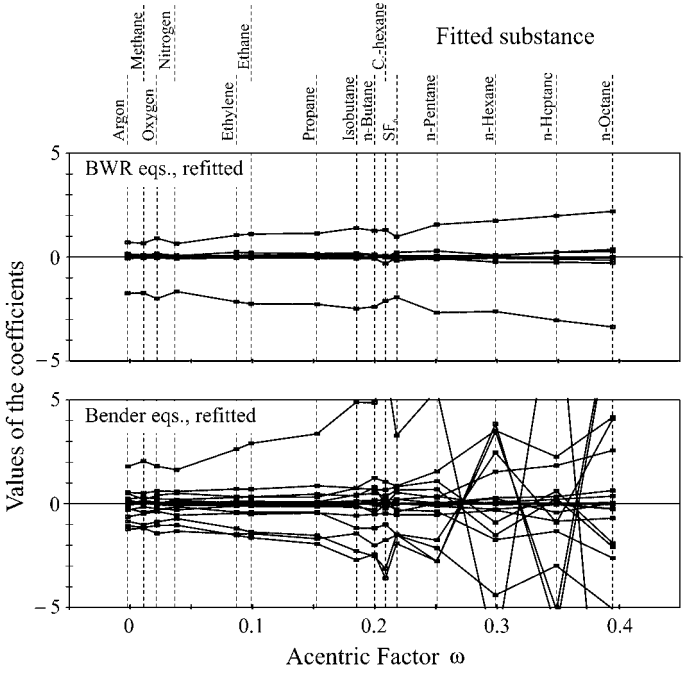

Fig. 4. Values of the coefficients of the BWR and Bender equations which resulted from fits to the data sets of the 15 non- and weakly polar fluids described in Ref. 15. The equations are written in reduced form, see Eq. (1). The coefficients are plotted over the acentric factor of the corresponding fluids.

derived caloric properties such as heat capacities or speeds of sound. Typical examples are the design of compressors, accounting of measured volume flows, or the optimization of processes with large throughput. In general, the accuracy of Bender equations which were fitted to data sets of well measured substances is regarded as sufficient for these kinds of applications. Problems may arise from some typical shortcomings of Bender equations, such as a poor representation of properties in the vapor region close to the saturation line or of liquid properties at low reduced temperatures. As far as possible, the new class of formulations should avoid these problems. Properties in the critical region should be reasonably represented, but in most cases there is no need for high accuracies in this area. The simplicity of the formulation was regarded as more important than a highly accurate representation of properties in the critical region. Based on this assessment, demands on the accuracy of calculated data for typical

Table I. Demands on the Accuracy of the New Class of Technical Equations of State

Pressure range	Uncertainty in $\rho(p,T)$	$w(p,T)$	$c_p(p,T)$	$p_s(T)$	$\rho'(T)$[g]	$\rho''(T)$[g]
$p \leqslant 30$ MPa[a]	0.2%[b]	1–2%[c]	1–2%[c]	0.2%[d]	0.2%	0.4%[d,e]
$p > 30$ MPa[f]	0.5%	2%	2%	–	–	–

[a] Larger uncertainties are to be expected in the extended critical region.
[b] In the extended critical region $\Delta p/p < 0.2\%$ is used instead of the demand given for $\Delta\rho/\rho$.
[c] 1% at gaseous and gas-like supercritical states, 2% at liquid and liquid-like states.
[d] Larger relative uncertainties can be tolerated for small vapor pressures and small saturated vapor densities.
[e] Combination of the uncertainties of gas densities and vapor pressures; experimental data of this accuracy are available for only a few substances.
[f] States at pressures $p > 100$ MPa are not considered due to their limited technical relevance.
[g] $'$ refers to saturated liquid states, $''$ to saturated vapor states.

thermal and caloric properties can be formulated; these demands are summarized in Table I.

However, the most important demands relate to the numerical stability of the formulations. Results for derived caloric properties such as heat capacities need to be reliable even if the equation could only be fitted to data for thermal properties. Fits to small data sets need to be possible to be able to establish equations for as many fluids as possible based on existing data sets and to reduce the experimental efforts which are necessary for an accurate description of fluids for which no sufficiently accurate data are available. Furthermore, it is essential that equations of state reasonably extrapolate beyond the range where they could be fitted to experimental data in many technical applications. This is especially true when applied to pure component equations in Helmholtz energy based mixture models [26] where properties may be calculated for reduced temperatures at which one or more of the involved pure substances is not in a physically and chemically stable fluid state at all.

3. SETTING UP EQUATIONS OF STATE FOR TECHNICAL APPLICATIONS

Modern equations of state which are intended to describe the whole range of fluid states of a pure substance are usually formulated in the reduced Helmholtz energy. The reduced Helmholtz energy is split into one part which describes the behavior of the hypothetical ideal gas (superscript o) at given values of temperature and density and a second part which

describes the residual behavior (superscript r) of the real fluid. Thus, the equation of state is written in the form

$$\frac{a(T, \rho)}{RT} = \frac{a^{\circ}(T, \rho) + a^{r}(T, \rho)}{RT} = \alpha^{\circ}(\tau, \delta) + \alpha^{r}(\tau, \delta), \tag{2}$$

where a is the specific or molar Helmholtz energy, R the corresponding gas constant, T the temperature, ρ the density, $\tau = T_r/T$ the inverse reduced temperature, and $\delta = \rho/\rho_r$ the reduced density. Since the Helmholtz energy as a function of temperature and density is one of the variable sets which are suitable for the formulation of so called fundamental equations, all thermodynamic properties can be calculated by combinations of derivatives of α° and α^{r} with respect to τ and δ. Table II summarizes the corresponding relations for some important properties.

The required relation for the ideal gas part, $\alpha^{\circ}(\tau, \delta)$, can easily be obtained from an integrable equation for the heat capacity of the ideal gas, $c_p^{\circ}(T)$, which is known rather accurately for many technically important fluids. The development of equations for $c_p^{\circ}(T)$ and the required integration is described in detail in Ref. 13. The work described here focuses on the description of the residual part of the reduced Helmholtz energy, $\alpha^{r}(\tau, \delta)$.

The decisive techniques which are required to establish formulations for $\alpha^{r}(\tau, \delta)$ are "weighting of the underlying experimental data," "linear and nonlinear multiproperty fitting," and "optimization of the functional form." The corresponding algorithms are basically known both with regard to their theoretical background (see, e.g., Refs. 27–29) and with regard to their practical application (see, e.g., Refs. 1 and 7). Those fundamentals will not be repeated at this point; for an overview see Refs. 13 and 30. However, compared to the completely substance-specific development of reference equations, some differences result from the application of the simultaneous optimization procedure by Span et al. [14] to equations of state for technical applications. These special requirements will be discussed in this section.

The general setup which was chosen for the new class of equations of state reads

$$\frac{a^{r}(T, \rho)}{RT} = \alpha^{r}(\tau, \delta) = \sum_{i=1}^{I_{Pol}+I_{Exp}} A_i(\tau, \delta)$$

$$= \sum_{i=1}^{I_{Pol}} n_i \tau^{t_i} \delta^{d_i} + \sum_{i=I_{Pol}+1}^{I_{Pol}+I_{Exp}} n_i \tau^{t_i} \delta^{d_i} \exp(-\delta^{p_i}). \tag{3}$$

Table II. Definitions of Common Thermodynamic Properties and Their Relation to the Reduced Helmholtz Energy α

Property and definition	Relation to α and its derivatives[a]
Pressure $p(T,\rho) = -(\partial a/\partial v)_T$	$\dfrac{p}{\rho RT} = 1 + \delta\alpha^{\mathrm{r}}_\delta$
Derivatives of pressure $(\partial p/\partial\rho)_T$ $(\partial p/\partial T)_\rho$	$(\partial p/\partial\rho)_T = RT(1 + 2\delta\alpha^{\mathrm{r}}_\delta + \delta^2\alpha^{\mathrm{r}}_{\delta\delta})$ $(\partial p/\partial T)_\rho = R\rho(1 + \delta\alpha^{\mathrm{r}}_\delta - \delta\tau\alpha^{\mathrm{r}}_{\delta\tau})$
Entropy $s(T,\rho) = -(\partial a/\partial T)_v$	$\dfrac{s}{R} = \tau(\alpha^{\mathrm{o}}_\tau + \alpha^{\mathrm{r}}_\tau) - \alpha^{\mathrm{o}} - \alpha^{\mathrm{r}}$
Internal energy $u(T,\rho) = a + Ts$	$\dfrac{u}{RT} = \tau(\alpha^{\mathrm{o}}_\tau + \alpha^{\mathrm{r}}_\tau)$
Isochoric heat capacity $c_v(T,\rho) = (\partial u/\partial T)_v$	$\dfrac{c_v}{R} = -\tau^2(\alpha^{\mathrm{o}}_{\tau\tau} + \alpha^{\mathrm{r}}_{\tau\tau})$
Enthalpy $h(T,p) = u + pv$	$\dfrac{h}{RT} = 1 + \tau(\alpha^{\mathrm{o}}_\tau + \alpha^{\mathrm{r}}_\tau) + \delta\alpha^{\mathrm{r}}_\delta$
Isobaric heat capacity $c_p(T,p) = (\partial h/\partial T)_p$	$\dfrac{c_p}{R} = -\tau^2(\alpha^{\mathrm{o}}_{\tau\tau} + \alpha^{\mathrm{r}}_{\tau\tau}) + \dfrac{(1 + \delta\alpha^{\mathrm{r}}_\delta - \delta\tau\alpha^{\mathrm{r}}_{\delta\tau})^2}{1 + 2\delta\alpha^{\mathrm{r}}_\delta + \delta^2\alpha^{\mathrm{r}}_{\delta\delta}}$
Speed of sound[b] $w(T,p) = \sqrt{(\partial p/\partial\rho)_s}$	$\dfrac{w^2}{RT} = 1 + 2\delta\alpha^{\mathrm{r}}_\delta + \delta^2\alpha^{\mathrm{r}}_{\delta\delta} - \dfrac{(1 + \delta\alpha^{\mathrm{r}}_\delta - \delta\tau\alpha^{\mathrm{r}}_{\delta\tau})^2}{\tau^2(\alpha^{\mathrm{o}}_{\tau\tau} + \alpha^{\mathrm{r}}_{\tau\tau})}$
Joule–Thomson coef. $\mu(T,p) = (\partial T/\partial p)_h$	$\mu R\rho = \dfrac{-(\delta\alpha^{\mathrm{r}}_\delta + \delta^2\alpha^{\mathrm{r}}_{\delta\delta} + \delta\tau\alpha^{\mathrm{r}}_{\delta\tau})}{(1 + \delta\alpha^{\mathrm{r}}_\delta - \delta\tau\alpha^{\mathrm{r}}_{\delta\tau})^2 - \tau^2(\alpha^{\mathrm{o}}_{\tau\tau} + \alpha^{\mathrm{r}}_{\tau\tau})(1 + 2\delta\alpha^{\mathrm{r}}_\delta + \delta^2\alpha^{\mathrm{r}}_{\delta\delta})}$
Second thermal virial coefficient $B(T) = \lim_{\rho\to 0}(\partial(p/(\rho RT))/\partial\rho)_T$	$B\rho_{\mathrm{r}} = \lim_{\delta\to 0}\alpha^{\mathrm{r}}_\delta$
Third thermal virial coefficient $C(T) = \frac{1}{2}\lim_{\rho\to 0}(\partial^2(p/(\rho RT))/\partial\rho^2)_T$	$C\rho_{\mathrm{r}}^2 = \lim_{\delta\to 0}\alpha^{\mathrm{r}}_{\delta\delta}$
Second acoustic virial coefficient[c] $\beta_{\mathrm{a}}(T) = \lim_{\rho\to 0}(\partial(w^2/(k^{\mathrm{o}}_s RT))/\partial\rho)_T$	$\beta_{\mathrm{a}}\rho_{\mathrm{r}} = \lim_{\delta\to 0}\left[2\alpha^{\mathrm{r}}_\delta - 2\dfrac{k^{\mathrm{o}}_s - 1}{k^{\mathrm{o}}_s}\tau\alpha^{\mathrm{r}}_{\delta\tau} + \dfrac{(k^{\mathrm{o}}_s - 1)^2}{k^{\mathrm{o}}_s}\tau^2\alpha^{\mathrm{r}}_{\tau\tau}\right]$
Liquid-vapor phase equilibrium[d] $T' = T'' = T_{\mathrm{s}}$ $p(T_{\mathrm{s}},\rho') = p(T_{\mathrm{s}},\rho'') = p_{\mathrm{s}}$ $g(T_{\mathrm{s}},\rho') = g(T_{\mathrm{s}},\rho'')$	Simultaneous solution of $\dfrac{p_{\mathrm{s}}}{RT_{\mathrm{s}}}\left(\dfrac{1}{\rho''} - \dfrac{1}{\rho'}\right) - \ln\left(\dfrac{\rho'}{\rho''}\right) = \alpha^{\mathrm{r}}(\tau_{\mathrm{s}},\delta') - \alpha^{\mathrm{r}}(\tau_{\mathrm{s}},\delta'')$ $\delta'(1 + \delta'\alpha^{\mathrm{r}}_\delta(\tau_{\mathrm{s}},\delta')) = \delta''(1 + \delta''\alpha^{\mathrm{r}}_\delta(\tau_{\mathrm{s}},\delta''))$

[a] $\alpha^{\mathrm{r}}_\delta = \left(\dfrac{\partial\alpha^{\mathrm{r}}}{\partial\delta}\right)_\tau$, $\alpha^{\mathrm{r}}_\tau = \left(\dfrac{\partial\alpha^{\mathrm{r}}}{\partial\tau}\right)_\delta$, $\alpha^{\mathrm{r}}_{\delta\delta} = \left(\dfrac{\partial^2\alpha^{\mathrm{r}}}{\partial\delta^2}\right)_\tau$, $\alpha^{\mathrm{r}}_{\tau\tau} = \left(\dfrac{\partial^2\alpha^{\mathrm{r}}}{\partial\tau^2}\right)_\delta$, $\alpha^{\mathrm{r}}_{\delta\tau} = \left(\dfrac{\partial^2\alpha^{\mathrm{r}}}{\partial\delta\,\partial\tau}\right)$, $\alpha^{\mathrm{o}}_\tau = \left(\dfrac{\partial\alpha^{\mathrm{o}}}{\partial\tau}\right)_\delta$, $\alpha^{\mathrm{o}}_{\tau\tau} = \left(\dfrac{\partial^2\alpha^{\mathrm{o}}}{\partial\tau^2}\right)_\delta$.

[b] The specific gas constant $R = R_{\mathrm{m}}/M$ has to be used to calculate speeds of sound.

[c] $k^{\mathrm{o}}_s = C^{\mathrm{o}}_p/C^{\mathrm{o}}_v$ is the isentropic expansion coefficient of the ideal gas.

[d] The index s indicates saturation, $'$ saturated liquid states, and $''$ saturated vapor states.

This form can be regarded as an advancement of the pressure-explicit form of the older modified BWR equations, Eq. (1). It was introduced by different groups (see, e.g., Refs. 7 and 8) in the 1980's and is well established for accurate empirical equations of state today.

Special terms for an improved description of properties in the critical region such as Gaussian bell-shaped terms (see Refs. 1–6) and nonanalytic terms (see Refs. 2 and 3) were not used in order to preserve the necessary simplicity of a technical equation of state. Such terms are unavoidable for highly accurate reference equations of state, but the demands which are defined in Table I can easily be satisfied without them.

Besides the polynomial and exponential terms in Eq. (3), we considered two different types of terms as promising candidates for use in technical equations of state. Expressions of the general form

$$A_i(\tau, \delta) = n_i \frac{\delta^{d_i} \tau^{t_i}}{(1 - c_i \delta)^2} \tag{4}$$

can be interpreted as an empirical simplification of the well known hard-sphere terms, see, e.g., Saager et al. [31]. The c_i introduced by such "*simplified hard-sphere terms*" are additional parameters, which have to be determined during the optimization process, and due to the quotient, the required derivatives become more complicated than the derivatives of Eq. (3). But compared to the original hard-sphere terms, the complications involved by Eq. (4) were still regarded as acceptable since terms like these were expected to improve the representation of properties at liquid and liquid-like supercritical states.

Tegeler et al. [32] derived "*square-well terms*" of the form

$$A_i(\tau, \delta) = n_i \delta^{d_i} (\exp(c_i \tau) - 1)^{m_i} \tag{5}$$

from an expression for the second virial coefficient which results from an integration of the square-well potential; see Mason and Spurling [33]. With c_i and m_i, Eq. (5) introduces two additional parameters and, compared to simple polynomial and exponential terms, derivatives with respect to τ become more complicated. Terms of this form were tested since they were expected to improve the representation of properties at gaseous and gas-like supercritical states.

However, neither simplified hard-sphere terms nor square-well terms resulted in a significant improvement of the resulting equations of state, and thus the general set-up of the "bank of terms," the pool of terms from which the optimization algorithm selects the functional form of the actual equation of state (see Refs. 13 and 29), was restricted to simple polynomial

and exponential terms. The final bank of terms used in the simultaneous optimization procedure contained a total of 583 terms and reads

$$\alpha^{\mathrm{r}}(\tau,\delta)=\sum_{i=1}^{8}\sum_{j=-8}^{12}n_{i,j}\,\delta^{i}\tau^{j/8}+\sum_{i=1}^{5}\sum_{j=-8}^{24}n_{i,j}\,\delta^{i}\tau^{j/8}\exp(-\delta)$$
$$+\sum_{i=1}^{5}\sum_{j=16}^{56}n_{i,j}\,\delta^{i}\tau^{j/8}\exp(-\delta^{2})+\sum_{i=2}^{4}\sum_{j=24}^{38}n_{i,j}\,\delta^{i}\tau^{j/2}\exp(-\delta^{3}), \tag{6}$$

with $\tau=T_{\mathrm{r}}/T$ and $\delta=\rho/\rho_{\mathrm{r}}$. To make use of a simple corresponding states similarity when using identical functional forms for a variety of substances, the reducing parameters T_{r} and ρ_{r} were chosen to be equal to the critical parameters T_{c} and ρ_{c}, or to the best estimated values available for T_{c} and ρ_{c} of the respective substance. Exponential expressions with density powers up to 6 were used in preliminary banks of terms, but the optimization algorithm did not select any of the corresponding terms—a restriction to terms up to $\exp(-\delta^3)$ seemed appropriate for simple technical equations of state.

With respect to the exponents used, Eq. (6) violates two of the recommendations given in Ref. 34 for functional forms resulting in a reasonable extrapolation behavior up to extreme temperatures and pressures. For pure polynomial terms, the use of density powers up to 8 (Ref. 34 asks for $i \leqslant 4$ for polynomial terms) leads to plots which are too steep in the limit of very high densities and affects the extrapolation to very high pressures. However, for technical equations of state with a restricted number of terms, the use of polynomials with high density powers is essential for an accurate representation of liquid properties, while the representation of properties at pressures of several giga pascals (GPa) can be regarded as arbitrary under technical aspects.

The use of negative exponents for the inversely reduced temperature τ results in virial coefficients which diverge at very high temperatures. When the bank of terms was defined, this shortcoming was accepted since terms with negative exponents for τ are generally expected to improve the representation of properties at low reduced temperatures. But at this point the experience with simultaneously optimized functional forms disproved common teachings—the final equations do not contain terms with negative exponents for τ, even though such terms were contained in the used bank of terms. If terms with negative exponents for τ had significantly improved the resulting equations of state in the low temperature range, where accurate data were contained in the used data sets, they would have been selected by the optimization algorithm.

3.1. Weighting of Experimental Data

In general, the use of weighted experimental data is recommended for the development of empirical correlation equations. For equations of state which are based on data for different properties, the use of weighted data becomes mandatory since deviations in different properties cannot be compared with each other unless they are normalized in a suitable way. Thus, the quality criterion of a multiproperty fit which considers data for P different properties becomes a sum of squares χ^2 which can be written as

$$\chi^2 = \sum_{p=1}^{P} \sum_{m=1}^{M_p} \frac{\zeta_{p,m}^2}{\sigma_{p,m,\exp}^2} = \sum_{p=1}^{P} \sum_{m=1}^{M_p} \frac{(y_{p,m,\exp} - y_{p,m,\mathrm{calc}})^2}{\sigma_{p,m,\exp}^2}. \tag{7}$$

In Eq. (7), y_p corresponds to the pth property or to a reduced form of the property and ζ_p to the corresponding residuum. M_p is the number of data used for the pth property and $\sigma_{p,m,\exp}^2$ is the variance which results from the experimental uncertainty of $y_{p,m,\exp}$. According to the law of error propagation, the variance $\sigma_{p,m,\exp}^2$ usually considers contributions from all measured quantities to assess the total uncertainty of a data point. For details see Ref. 13.

Compared to the development of reference equations of state which are expected to represent all data within their experimental uncertainty, an important difference results from the requirements formulated for the new class of technical equations of state in Section 2. When developing technical equations of state, highly accurate data are overemphasized if they are weighted with their experimental uncertainty. A $p\rho T$ data point m with $\sigma_{\rho,m,\exp}/\rho_m \approx 0.02\%$ would contribute $\zeta_m^2/\sigma_{\rho,m,\exp} \approx 100$ to the sum of squares for the corresponding substance when being represented just within the limit of $|\Delta\rho|/\rho = 0.2\%$. At higher temperatures for example, a less accurate data point j with $\sigma_{\rho,j,\exp}/\rho_j \approx 0.1\%$ would contribute only $\zeta_j^2/s_{\rho,j,\exp} \approx 4$ to the sum of squares when being represented also within $|\Delta\rho|/\rho = 0.2\%$. As a consequence, regions where highly accurate data are available would be overfitted while regions with worse, but sufficiently accurate data, would not be considered appropriately. To avoid this problem, experimental data had to be weighted with the demanded uncertainties summarized in Table I. Isochoric heat capacities, heat capacities at saturation and isobaric enthalpy differences were treated like isobaric heat capacities. Larger uncertainties were accepted for caloric properties in the critical region. Data for the Joule–Thomson coefficient and for non-isobaric enthalpy changes had to be assessed on an individual basis. Selected data for the second virial coefficient were used with $\sigma_B \simeq 0.02 \cdot B(T)$ for substances for which the data situation in the gas phase is poor. Data for

the second virial coefficient were not considered for most substances with a well measured gas phase.

In this way, the contribution to the sum of squares becomes 1 for data which are represented just within the demanded accuracy. The weighted variance of a fit,

$$\sigma_{\mathrm{wt}}^2 = \{\chi^2/(M-I)\} \cong \{\chi^2/M\} \tag{8}$$

with M the number of data points used and I the number of adjustable coefficients, becomes a measure for the fulfillment of the demands on accuracy. Only data with experimental uncertainties exceeding the requested uncertainty of the equation have to be weighted with their experimental uncertainty, if no more reliable data are available in the respective region.

Besides the individual weights for each data point, the application of the simultaneous optimization algorithm by Span et al. [14] requires a substance-specific reference sum of squares, $\chi_{\mathrm{o},j}^2$, for each of the J considered substances to build the quality criterion of the simultaneous optimization,

$$\mathrm{X}^{*2} = \sum_{j=1}^{J} \chi_j^{*2} = \sum_{j=1}^{J} \frac{\chi_j^2}{\chi_{\mathrm{o},j}^2}. \tag{9}$$

The reference sums of squares were determined by fitting nine-term equations of state which were established for each of the considered substances using a substance-specific optimization algorithm (see Ref. 29). The only criterion which was considered during the optimization of the equations was the achieved sum of squares. For substances with restricted data sets, these equations show all kinds of shortcomings which are expected for functional forms optimized on the basis of insufficient data sets. However, since they were needed only as a measure for the sums of squares which can be achieved by substance-specific optimization, the shortcomings of the nine-term equations do not affect the simultaneous optimization procedure in any way.

3.2. Critical Parameters

Reference equations of state are usually constrained to preselected values of the critical parameters T_c, ρ_c, and p_c in order to guarantee an exact representation of the critical point, to improve the representation of properties in the critical region, and to enable a reasonable application of special critical region terms which introduce differences $T-T_c$ and $\rho-\rho_c$ as

variables. However, it was decided not to constrain the new class of technical equations of state to preselected critical points for two reasons.

Preliminary equations which were constrained to preselected critical points needed 1 to 2 additional terms to fulfill the requirements outside the extended critical region. Since an exact representation of critical parameters is usually not important for technical applications, this additional numerical expense was regarded as not justified.

In general, accurate data for critical properties are available only for rather well measured substances. When setting up equations of state for technically important substances with restricted data sets, one often has to rely either on questionable experimental results for the critical properties or on predicted values. To estimate uncertainties of predicted critical properties for fluids in the class of equations of state presented here, 26 algorithms for the determination of critical parameters of *n*-alkanes, 12 algorithms for isomers of alkanes, 17 algorithms for alcohols, and 13 algorithms for other organic substances were tested. In general, algorithms based on group contribution methods were considered; for *n*-alkanes and alcohols, simple methods based on the number of carbon atoms or on the molar mass were considered as well. For the 18 *n*-alkanes from methane to octadecane, 15 isomers with 4 to 8 carbon atoms, 20 alcohols ranging from methanol to decanol, and 22 organic substances belonging to the groups of cyclo-alkanes, of aromatic substances, and of unsaturated hydrocarbons, deviations between experimental and predicted results for the critical parameters were investigated. The results are summarized in Table III for each of the groups for the algorithms which led to the smallest deviations. If the normal boiling temperature and the saturated liquid density at this state are accepted as additional parameters, the algorithm proposed by Vetere [38] yields slightly better results in many cases. However, based on these results, it became obvious that none of the algorithms is able to predict critical parameters with the accuracy that is required to represent, e.g., $p\rho T$ data in the extended critical region within $|\Delta p|/p \leqslant 0.2\%$; see Table I. The representation of properties in the homogeneous region could even be distorted if an equation of state is constrained to uncertain critical parameters.

For substances for which no reliable data are available in the critical region or at supercritical states, estimates for the critical temperature are usually the most accurate information on the location of the critical point. To make use of this information, estimated values for one saturated vapor ($\rho'' \approx 0.9\rho_{c,\,est}$) and one saturated liquid density ($\rho' \approx 1.1\rho_{c,\,est}$) close to the critical point ($T \approx 0.9998T_{c,\,est}$) can be introduced into the corresponding data set with very low weights ($\sigma_{\rho',\,\rho''}/\rho \approx 0.1$). In this way, the equation of state will yield reasonable critical parameters, which are consistent with the

Table III. Average and Maximum Deviations Between Experimentally Determined and Predicted Values for Critical Parameters

Group of substances	Reference	Average deviations (RMS[a]) T_c (%)	p_c (%)	ρ_c (%)	Maximum deviations T_c (%)	p_c (%)	ρ_c (%)
n-Alkanes	Teja et al. [35][b]	0.07	0.72	0.50	0.15	−2.15	−1.20
	Riedel [36][c]	0.23	3.01	7.04[d]	0.24	−3.67	−10.4[d]
Isomers	Riedel [36][c]	0.24	2.00	1.36	0.73	−3.42	−2.64
Alcohols	Teja et al. [35][b]	0.09	0.39	1.36	−0.16	−0.79	2.84
	Somayajulu [37][c]	1.06	2.96	2.78	−4.45	6.54	−6.59
Others	Somayajulu [37][c]	0.30	1.59	2.42	0.74	−3.14	7.09

[a] Root-mean-square deviation, $\mathrm{RMS} \equiv [\sum (100(y_{calc} - y_{exp})/y_{exp})^2/M^2]^{0.5}$.
[b] Based on the number of carbon atoms in a molecule.
[c] Based on a group contribution method.
[d] Large deviations due to more recent findings regarding the critical density of higher alkanes.

experimental information available for saturated and homogeneous states. However, for fluids with uncertain critical parameters, experimental data in the extended critical region are generally scarce and the functional forms presented here were not designed for an accurate prediction of properties in the critical region. Thus, the critical parameters of the equation should not be used as the best approximation for the "true" critical parameters. The influence of uncertain critical parameters on the accuracy of the equation of state outside of the critical region will be discussed in Section 3.3.2.

For the considered fluids, the resulting equations yield critical temperatures which generally agree with the "true values" of T_c within a few tenths of a kelvin. The deviations with respect to the critical pressure and density remain within the limits which can be deduced from the deviation in T_c and from the demands on the accuracy of properties in the homogeneous region. Details on the resulting critical parameters are given in subsequent articles [15, 16] together with further substance-specific information.

3.3. Accuracy Versus Numerical Stability

Based on the foundations explained above and on carefully weighted data sets for 15 non- and weakly polar fluids and for 13 typical polar fluids,[4] the simultaneous optimization algorithm was used to establish functional forms for technical equations of state for non- and weakly polar fluids and for typical polar fluids. It was found that equations of state

[4] For homogeneous states, the final data sets contain almost 55,000 experimental data points, which were selected out of a total of more than 100,000 data points. For details see Refs. 15 and 16.

based on simultaneously optimized functional forms with 10 terms are generally able to satisfy the demands summarized in Table I. These equations resulted in weighted variances below one for all considered fluids except for the associating fluid ammonia, and on average they are superior to the results of refitted Bender equations of state [18] with 19 terms. However, in certain regions, the 10-term equations fail to strictly fulfill the formulated demands. Caloric properties and especially speeds of sound for liquid states at low reduced temperatures are frequently represented with relative deviations significantly larger than $\pm 2\%$. With regard to the representation of thermal properties, shortcomings are found for high density gaseous states and at supercritical states especially for equations based on the functional form for polar fluids. Functional forms with 11 terms do not result in significant improvements. Functional forms with 12 terms are needed to strictly fulfill the formulated demands except for very few points where enlarged deviations are observed for different reasons; these exceptions will be discussed in subsequent articles [15, 16] in detail.

Typical examples of the shortcomings of equations of state based on simultaneously optimized functional forms with 10 terms and for the superiority of those based on functional forms with 12 terms are shown in Figs. 5 and 6. Figure 5 shows the representation of accurate speed of sound

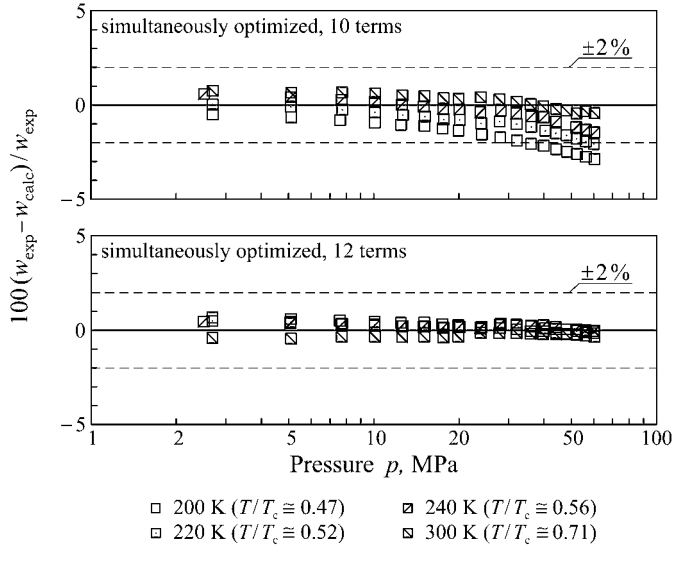

Fig. 5. Percentage deviations between experimental data for the speed of sound in the liquid phase of normal butane measured by Niepmann [24] and values calculated from simultaneously optimized equations of state with 10 and 12 terms.

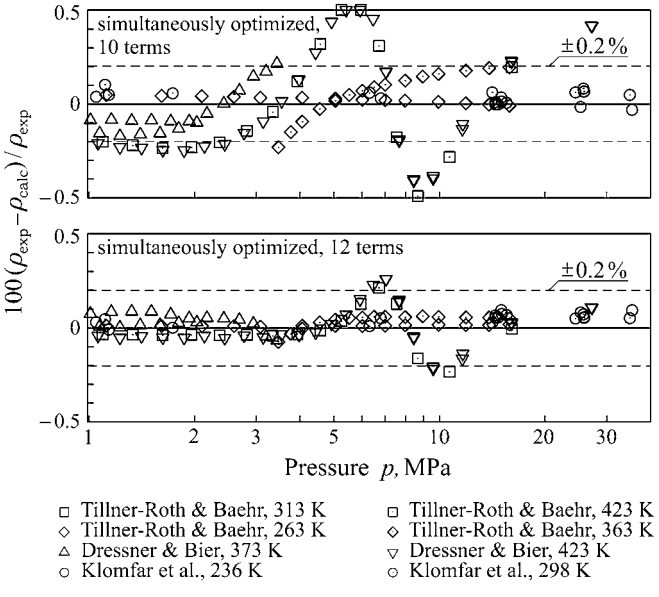

Fig. 6. Percentage deviations between experimental results for the density of R134a by Tillner-Roth and Baehr [39, 40], Dressner and Bier [41] and Klomfar et al. [42] and values calculated from simultaneously optimized equations of state with 10 and 12 terms.

data in the liquid phase of *n*-butane; see Fig. 2 for comparison. At temperatures above 220 K ($T/T_c \approx 0.52$), the equation of state which is based on the functional form for non- and weakly polar fluids with 10 terms is able to represent the speed of sound data by Niepmann [24] within $|\Delta w|/w \leqslant 2\%$. However, at lower temperatures, the observed deviations clearly exceed this limit. The equation based on the functional form for non- and weakly polar fluids with 12 terms represents all of the data within the demanded accuracy.

Figure 6 shows deviations between selected experimental data for the density of 1,1,1,2-tetrafluoroethane (HFC-134a) and values calculated from equations of state based on simultaneously optimized functional forms for polar fluids with 10 and 12 terms. The equation with 12 terms represents most of the data within $|\Delta\rho|/\rho \leqslant 0.2\%$. Those data which exceed this limit represent states in the extended critical region; the corresponding deviations in pressure remain within $|\Delta p|/p \leqslant 0.2\%$. The equation with 10 terms represents most data within $|\Delta\rho|/\rho \leqslant 0.2\%$ as well, but it cannot strictly satisfy the formulated demands on accuracy. In this example, enlarged deviations are observed for supercritical states over the whole range of investigated pressures.

Based strictly on the demands formulated in Table I, one has to conclude that simultaneously optimized functional forms with 12 terms form the ideal basis for the new class of technical equations of state. However, simultaneously optimized equations with only 10 terms are numerically more stable than those with 12 terms. This fact is illustrated in Fig. 7, which shows the plots of the coefficients resulting from independent fits to data sets for 15 non- and weakly polar fluids over the acentric factor; see Fig. 4 for comparison. The coefficients of the equations using the simultaneously optimized functional form with 10 terms are small, and the values of the coefficients are smooth functions of the acentric factor of the fluid. Significant oscillations are not observed. The plots which result from the functional form with 12 terms still indicate higher numerical stability than those found for the BWR equation with only 8 terms and far inferior accuracy. In general the values of the coefficients do not change rapidly from substance to substance. However, the observed oscillations and intercorrelations are clearly more pronounced than for the equation with 10 terms.

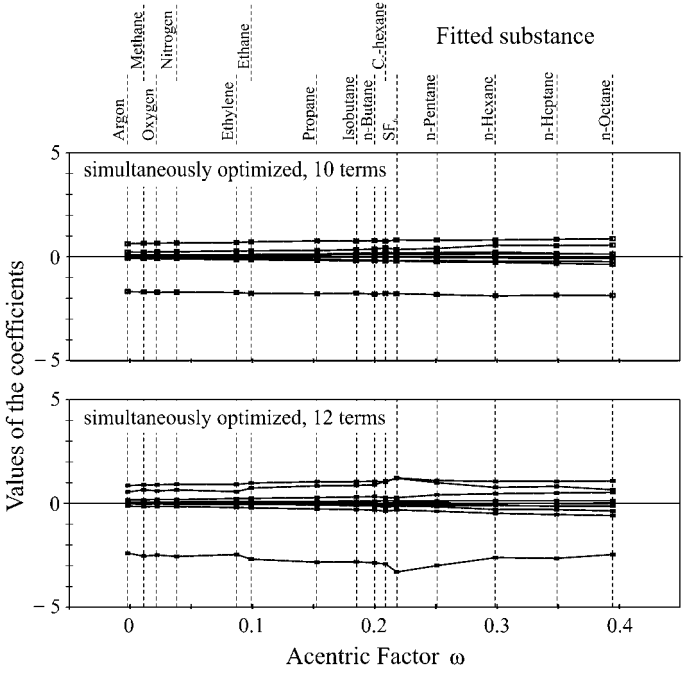

Fig. 7. Values of the coefficients of equations of state based on simultaneously optimized functional forms with 10 and 12 terms. The coefficients resulted from fits to the data sets of 15 non- and weakly polar fluids described in Ref. 15. The coefficients are plotted over the acentric factor of the corresponding fluids.

The major objective of this project was to establish functional forms for sufficiently accurate equations of state for typical nonpolar and polar fluids which can be transferred easily to technically important substances with small data sets. Bearing in mind this fact and the results shown in Fig. 7, it had to be clarified whether the obvious advantages of equations with 12 terms do not turn into disadvantages in practice when being fitted to small data sets.

3.3.1. Investigation of Numerical Stability

The numerical stability of a functional form can be tested systematically by comparisons with well defined data sets calculated from highly accurate reference equations or by an investigation of equations of state which were fitted to subaverage data sets. The second approach is informative especially if additional data become available in regions which were not covered by data when the corresponding equation was fitted.

For a systematic investigation of numerical stability, values for the density, the isobaric heat capacity and the speed of sound of methane were calculated from the highly accurate reference equation by Setzmann and Wagner [1] at 511 points. The established data set covers temperatures from 95 to 450 K ($T_t = 90.6941$ K and $T_c = 190.564$ K) and pressures up to 100 MPa at reasonable intervals, including gaseous, liquid, critical, and supercritical states. Additionally, data for the vapor pressure and the saturated vapor and liquid density were calculated at 20 temperatures.

In a first step, equations of state with simultaneously optimized functional forms with 10 and 12 terms were fitted to the complete data set, considering data of all properties. For homogeneous states, Fig. 8 reports the resulting percentage absolute average deviations

$$\mathrm{AAD} \equiv \sum_{m=1}^{M} (100\,|\Delta y_m|/y_m)/M \tag{10}$$

under the heading "complete data set." To make the comparison more expressive, six regions are defined in Fig. 8: gas, liquid, (extended) critical region, and supercritical fluid with low densities (LD, $\rho \leqslant 0.6\rho_c$), medium densities (MD, $0.6\rho_c < \rho < 1.5\rho_c$), and high densities (HD, $\rho \geqslant 1.5\rho_c$). In the extended critical region, pressure deviations are used instead of density deviations. As was to be expected, both equations yield average absolute deviations which are smaller than the demanded uncertainties when being fitted to the complete data sets. The equation with 12 terms is superior to the equation with 10 terms in all regions and for all properties.

In a second step, both equations were fitted to a reduced data set which consisted of 21 $p\rho T$ data in the range $100\,\mathrm{K} \leqslant T \leqslant 300\,\mathrm{K}$ and

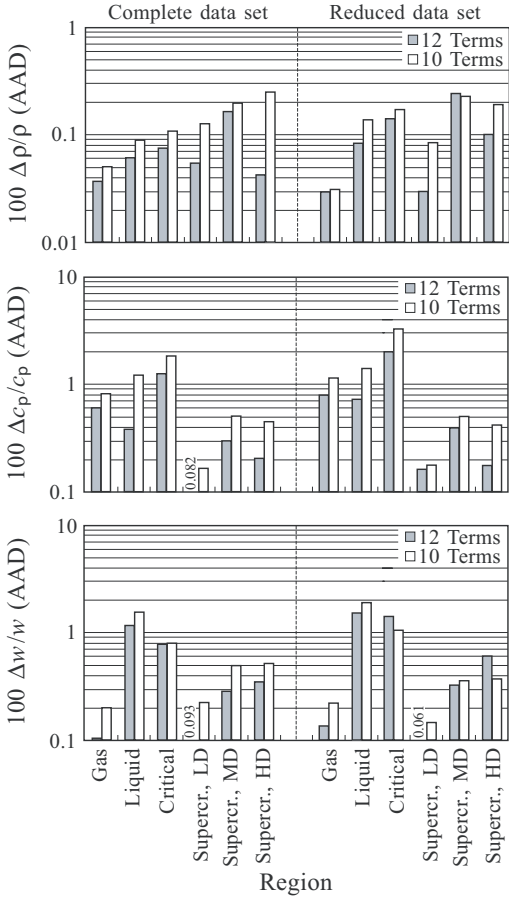

Fig. 8. Average absolute deviations between densities, isobaric heat capacities, and speeds of sound calculated from simultaneously optimized equations with 10 and 12 terms and from the reference equation by Setzmann and Wagner [1]. See the text for an explanation of the different supercritical regions. In the critical region, pressure deviations are used instead of density deviations.

$p \leqslant 95$ MPa, 4 vapor pressures and 4 saturated liquid densities in the range $100\ \mathrm{K} \leqslant T \leqslant 185\ \mathrm{K}$ and 2 saturated vapor densities at temperatures of 160 and 185 K. To imitate a small but accurate set of experimental data, a normally distributed scatter with a standard deviation of $\sigma_y = 0.02\%$ was added to the calculated values. Under the heading "reduced data set," Fig. 8 summarizes the results of comparisons between the data *which were not*

used in the fit and values predicted from the simultaneously optimized equations of state. For the 12-term equation which was fitted to such an extremely small data set consisting only of 31 data for thermal properties, the observed average absolute deviations exceed the demanded uncertainties only slightly in a single region, namely for the representation of $p\rho T$ data at supercritical states with medium densities. The advantages of the equation with 12 terms are less pronounced than before, but still the longer equation yields better results. When being fitted to such small data sets, multiparameter equations of state without an optimized functional form yield unphysical results especially for derived caloric properties.

Systematic investigations like the one described above prove the superior numerical stability of equations of state with a simultaneously optimized functional form. There were no obvious indications of disadvantages of functional forms with 12 terms.

When setting up the new class of technical equations for nonpolar and polar fluids, simultaneously optimized functional forms had to be fitted to very restricted data sets especially for the higher alkanes. For *n*-heptane and *n*-octane, reliable data were available only for liquid states; see the discussion in Ref. 15. For the representation of properties in the gas phase and at supercritical states, we could rely only on some questionable data for the second virial coefficient and on the numerical stability of the used functional forms. As a very sensitive test for the extrapolation behavior of the resulting equations, Fig. 9 shows plots of the ideal curves of *n*-octane calculated from simultaneously optimized equations of state with 10 and 12 terms and from a Bender equation; for details on the definition of these curves see Refs. 13 and 34. The equations with simultaneously optimized functional forms show qualitatively correct plots with only slight oscillations even for the outermost curve, the Joule inversion curve. This result agrees with very reasonable plots found for thermal properties as well as for derived caloric properties—the "theoretically expected" plots in Fig. 3 were calculated from the simultaneously optimized equation with 12 terms. Similar results can be found for other polar and nonpolar substances as well. Figure 10 shows Joule–Thomson and Joule inversion curves calculated from simultaneously optimized equations of state with 12 terms for methane, propane, *n*-pentane, and *n*-heptane. Slight deformations become obvious only for *n*-heptane. Although the corresponding equation is based almost exclusively on liquid data, it still predicts a qualitatively correct plot even of the Joule inversion curve. For an assessment of the performance of simultaneously optimized equations, one has to be aware that only very few reference equations for substances with extensive data sets have so far been able to predict Joule inversion curves at least qualitatively correctly; see Ref. 34.

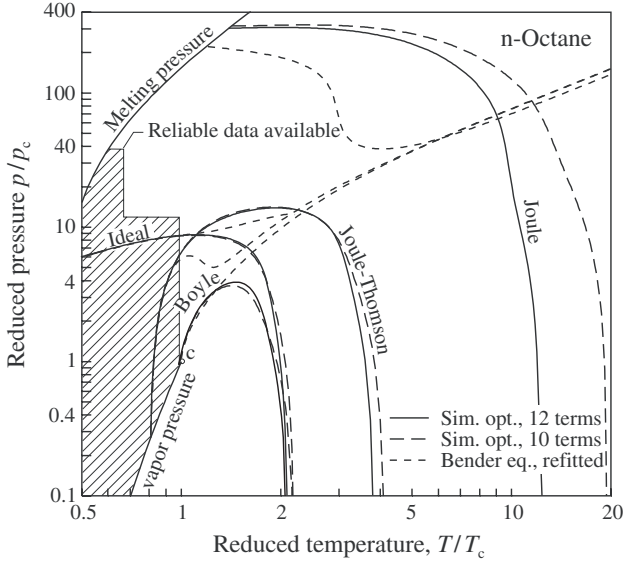

Fig. 9. Ideal curves of *n*-octane calculated from simultaneously optimized equations of state with 10 and 12 terms and from a refitted Bender equation. The hatched area corresponds to the region where reliable data were available to fit the equations.

Experimental investigations of the isochoric heat capacity at gaseous, liquid, critical, and supercritical states by Abdulagatov [43] became available both for *n*-heptane and *n*-octane after the work on the corresponding equations had been finished. For gaseous, critical, and supercritical states, the representation of these data can be regarded as purely predictive, since data had not been available in these regions either for thermal or for caloric properties. At liquid states, data for thermal and caloric properties, but not for the isochoric heat capacity, had been previously available. Figure 11 shows the representation of data on isochores with gas-like, almost critical, and liquid-like densities. In the extended critical region, the deviations between experimental data and predicted heat capacities exceed $|\Delta c_v|/c_v = 5\%$; this result was expected since simple technical equations cannot follow the steep increase of the isochoric heat capacity in this region. However, outside the extended critical region, the heat capacities are generally predicted within $|\Delta c_v|/c_v = 2\%$ and thus within the uncertainty claimed for this property.

The numerical stability of equations of state which use simultaneously optimized functional forms with 12 terms is obviously sufficient for the

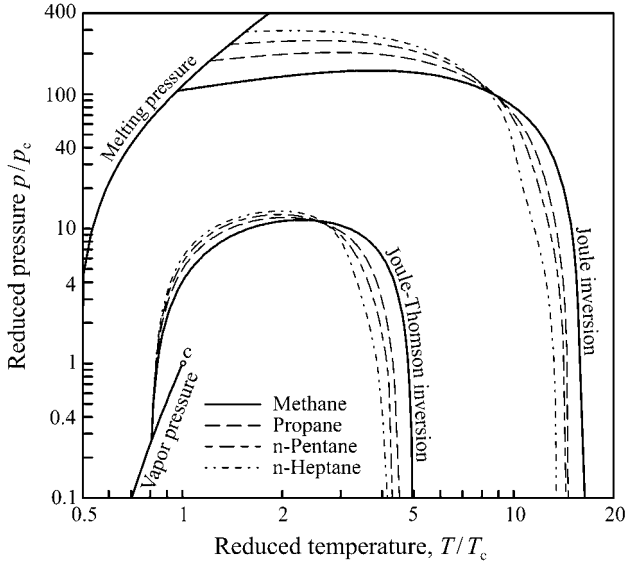

Fig. 10. Joule–Thomson and Joule inversion curves of methane, propane, *n*-pentane, and *n*-heptane calculated from simultaneously optimized equations of state with 12 terms. The plotted phase boundaries correspond to those of methane.

applications they were developed for. Functional forms with 10 terms are numerically more stable, but they yield worse results for the considered thermodynamic properties even when fitted to restricted data sets.

3.3.2. The Influence of Uncertain Critical Parameters

For reasons which were discussed in Section 3.2, the new equations for technical applications were not constrained to certain critical parameters and thus the influence of uncertain values for T_c, p_c, and ρ_c is reduced drastically. However, values for T_c and ρ_c are still needed as reducing parameters in Eq. (6) and in the resulting equations of state.

When using only simple polynomial and exponential terms, faulty values for T_c do not result in changes regarding the representation of thermodynamic properties. If τ is reduced with a critical temperature T_c^* instead of the "true" critical temperature T_c, the coefficients of the equation become

$$n_i^* = n_i \left(\frac{T_c}{T_c^*} \right)^{t_i} \tag{11}$$

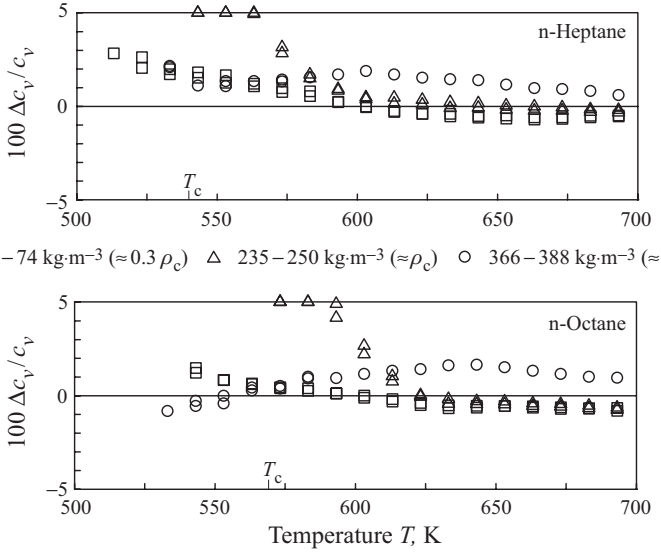

Fig. 11. Percentage deviations $100(c_{v,\,\mathrm{calc}}-c_{v,\,\mathrm{exp}})/c_{v,\,\mathrm{exp}}$ between experimental data for the isochoric heat capacity of *n*-heptane and *n*-octane by Abdulagatov [43] and values predicted by the corresponding simultaneously optimized equations of state with 12 terms.

and calculations are not affected at all. Due to the set-up of the exponential functions in Eq. (6), this does not hold for faulty critical densities ρ_c^*, but most of the influence can still be compensated for by changing the coefficients.

In Section 3.2 it was shown that uncertainties of 3% are typical for critical densities of substances for which no accurate experimental results are available for the critical properties. Errors up to $\pm 10\%$ may be encountered in some cases. To assess the effect of such uncertainties, simultaneously optimized equations of state with 10 and 12 terms have been fitted to the complete data set for propane, where the density has been reduced with $\rho_r = 0.9 \cdot \rho_c$, $\rho_r = 0.97 \cdot \rho_c$, $\rho_r = \rho_c$, $\rho_r = 1.03 \cdot \rho_c$, and $\rho_r = 1.1 \cdot \rho_c$. The results of this test are summarized in Fig. 12 for the functional form with 12 terms. The indicated regions correspond to those defined in Section 3.3.1.

The best results were found for $\rho_r = \rho_c$, the case which was assumed when optimizing the functional form. However, changes of $|\Delta\rho_r|/\rho_c = 3\%$ had hardly any effect on the accuracy of the resulting equations. The

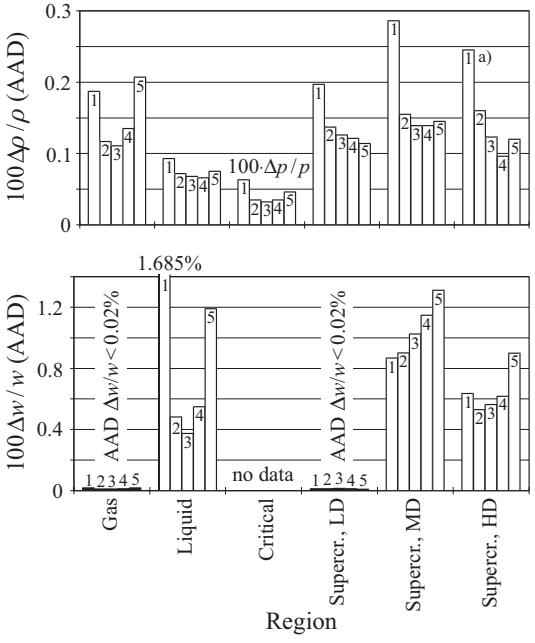

1: $\rho_r = 0.9\,\rho_c$ 2: $\rho_r = 0.97\,\rho_c$ 3: $\rho_r = \rho_c$ 4: $\rho_r = 1.03\,\rho_c$ 5: $\rho_r = 1.1\,\rho_c$

[a] Mostly states at $p > 30$ MPa with a claimed uncertainty of $|\Delta\rho|/\rho = 0.5\%$; see Table I.

Fig. 12. Percentage average absolute deviations resulting from fits to propane data for simultaneously optimized equations of state with 12 terms and different reducing densities.

observed average deviations are still far smaller than the demanded uncertainties. Changes of $|\Delta\rho_r|/\rho_c = 10\%$ resulted in significantly worse equations of state. The average deviations are still smaller than the demanded uncertainties, except for $p\rho T$ data in the gas phase for $\rho_r = 1.1\rho_c$ and at supercritical states with medium densities for $\rho_r = 0.9\rho_c$, but the maximum deviations exceeded the demanded uncertainties in other regions as well.

However, an uncertainty of 10% in the critical density generally only occurs for uncommon substances with very restricted data sets. In this sense, the results summarized in Fig. 12 prove that typical uncertainties of critical parameters are no threat for technical equations of state based on simultaneously optimized functional forms. Simultaneously optimized equations with 10 terms are slightly more sensitive to changes in ρ_r; thus, the uncertainty of critical parameters does not go against functional forms with 12 terms in any way.

4. THE FINAL FUNCTIONAL FORMS

Based on the results described in Section 3.3, functional forms with a total of 12 polynomial and exponential terms were established as a basis for technical equations of state for the group of non- and weakly polar fluids and for the group of typical polar fluids. In this section, the final functional forms are given together with some global assessments of their quality. Substance-specific details on the new class of technical equations of state are given in subsequent articles for non- and weakly polar fluids [15] and for typical polar fluids [16].

4.1. Results for Non- and Weakly Polar Fluids

Data sets for a total of 15 non- and weakly polar substances were considered when working on a simultaneously optimized functional form for these fluids. The critical temperatures of the fluids considered in comparisons and in the optimization procedure covered the range from $T_c = 126.192$ K for nitrogen and $T_c = 150.791$ K for argon, respectively, to $T_c = 569.32$ K for *n*-octane. The acentric factors cover the range from $\omega \approx -0.002$ for argon to $\omega \approx 0.391$ for *n*-octane. At low reduced temperatures, experimental data were considered down to the triple point of propane at $T_t/T_c \approx 0.231$. At high reduced temperatures, data were considered up to the limits which result from the experimental data which are available for argon ($T_{max}/T_c \approx 3.45$) and nitrogen ($T_{max}/T_c \approx 8.51$). Data at pressures above $p_{max} \approx 100$ MPa were not considered due to the limited technical relevance of extremely high pressures.

Based on selected data sets for methane, ethane, propane, *n*-butane, *n*-hexane, *n*-heptane, *n*-octane, argon, oxygen, ethylene, isobutane, cyclohexane, and sulfur hexafluoride and on the bank of terms given as Eq. (6), the simultaneous optimization algorithm resulted in the following functional form for technical equations of state for non- or weakly polar fluids:

$$\begin{aligned}\alpha(\tau,\delta) &= \alpha^{o}(\tau,\delta)+\alpha^{r}(\tau,\delta)\\ &= \alpha^{o}(\tau,\delta)+n_1\delta\tau^{0.250} \quad +n_2\delta\tau^{1.125} \quad +n_3\delta\tau^{1.500}\\ &\quad +n_4\delta^2\tau^{1.375} \quad +n_5\delta^3\tau^{0.250} \quad +n_6\delta^7\tau^{0.875}\\ &\quad +n_7\delta^2\tau^{0.625}e^{-\delta} \quad +n_8\delta^5\tau^{1.750}e^{-\delta} \quad +n_9\delta\tau^{3.625}e^{-\delta^2}\\ &\quad +n_{10}\delta^4\tau^{3.625}e^{-\delta^2}+n_{11}\delta^3\tau^{14.5}e^{-\delta^3}+n_{12}\delta^4\tau^{12.0}e^{-\delta^3}, \qquad (12)\end{aligned}$$

with the reduced Helmholtz energy $\alpha = a/(RT)$, the temperature T, the gas constant R, the inverse reduced temperature $\tau = T_c/T$, and the reduced density $\delta = \rho/\rho_c$. The substance-specific parameters T_c, ρ_c, R, and n_i which

are needed to evaluate Eq. (12) and the sources of the correlations used for the ideal gas contribution, $a^{\circ}(\tau, \delta)$, are given in Ref. 15. The derivatives of Eq. (12) which are needed to calculate common thermodynamic properties are summarized in Table IV. The data sets for *n*-pentane and nitrogen were used to test the applicability of Eq. (12) to other non- or weakly-polar fluids—no significant disadvantages were found for the representation of the data which are available for these substances, even though the data set for nitrogen covers a broader range of reduced temperatures than all data sets used in the simultaneous optimization procedure.

Table IV. Derivatives of Eqs. (12) and (13) for the Residual Part of the Helmholtz Energy with Respect to τ and δ

Derivative, abbreviation, and formulation in τ and δ

$$\alpha^{\mathrm{r}} = \sum_{i=1}^{I_{\mathrm{Pol}}} n_i \delta^{d_i} \tau^{t_i} + \sum_{i=I_{\mathrm{Pol}}+1}^{I_{\mathrm{Pol}}+I_{\mathrm{Exp}}} n_i \delta^{d_i} \tau^{t_i} \exp(-\delta^{p_i})$$

$$\left(\frac{\partial \alpha^{\mathrm{r}}}{\partial \delta}\right)_{\tau} = \alpha^{\mathrm{r}}_{\delta} = \sum_{i=1}^{I_{\mathrm{Pol}}} n_i d_i \delta^{d_i-1} \tau^{t_i} + \sum_{i=I_{\mathrm{Pol}}+1}^{I_{\mathrm{Pol}}+I_{\mathrm{Exp}}} n_i \delta^{d_i-1} (d_i - p_i \delta^{p_i})\, \tau^{t_i} \exp(-\delta^{p_i})$$

$$\left(\frac{\partial^2 \alpha^{\mathrm{r}}}{\partial \delta^2}\right)_{\tau} = \alpha^{\mathrm{r}}_{\delta\delta} = \sum_{i=1}^{I_{\mathrm{Pol}}} n_i d_i (d_i - 1)\, \delta^{d_i-2} \tau^{t_i}$$

$$+ \sum_{i=I_{\mathrm{Pol}}+1}^{I_{\mathrm{Pol}}+I_{\mathrm{Exp}}} n_i \delta^{d_i-2} ((d_i - p_i \delta^{p_i})(d_i - 1 - p_i \delta^{p_i}) - p_i^2 \delta^{p_i})\, \tau^{t_i} \exp(-\delta^{p_i})$$

$$\left(\frac{\partial \alpha^{\mathrm{r}}}{\partial \tau}\right)_{\delta} = \alpha^{\mathrm{r}}_{\tau} = \sum_{i=1}^{I_{\mathrm{Pol}}} n_i t_i \delta^{d_i} \tau^{t_i-1} + \sum_{i=I_{\mathrm{Pol}}+1}^{I_{\mathrm{Pol}}+I_{\mathrm{Exp}}} n_i t_i \delta^{d_i} \tau^{t_i-1} \exp(-\delta^{p_i})$$

$$\left(\frac{\partial^2 \alpha^{\mathrm{r}}}{\partial \tau^2}\right)_{\delta} = \alpha^{\mathrm{r}}_{\tau\tau} = \sum_{i=1}^{I_{\mathrm{Pol}}} n_i t_i (t_i - 1)\, \delta^{d_i} \tau^{t_i-2} + \sum_{i=I_{\mathrm{Pol}}+1}^{I_{\mathrm{Pol}}+I_{\mathrm{Exp}}} n_i t_i (t_i - 1)\, \delta^{d_i} \tau^{t_i-2} \exp(-\delta^{p_i})$$

$$\left(\frac{\partial^2 \alpha^{\mathrm{r}}}{\partial \delta\, \partial \tau}\right) = \alpha^{\mathrm{r}}_{\delta\tau} = \sum_{i=1}^{I_{\mathrm{Pol}}} n_i d_i t_i \delta^{d_i-1} \tau^{t_i-1} + \sum_{i=I_{\mathrm{Pol}}+1}^{I_{\mathrm{Pol}}+I_{\mathrm{Exp}}} n_i t_i \delta^{d_i-1} (d_i - p_i \delta^{p_i})\, \tau^{t_i-1} \exp(-\delta^{p_i})$$

$$\left(\frac{\partial^3 \alpha^{\mathrm{r}}}{\partial \delta\, \partial \tau^2}\right) = \alpha^{\mathrm{r}}_{\delta\tau\tau} = \sum_{i=1}^{I_{\mathrm{Pol}}} n_i d_i t_i (t_i - 1)\, \delta^{d_i-1} \tau^{t_i-2}$$

$$+ \sum_{i=I_{\mathrm{Pol}}+1}^{I_{\mathrm{Pol}}+I_{\mathrm{Exp}}} n_i t_i (t_i - 1)\, \delta^{d_i-1} (d_i - p_i \delta^{p_i})\, \tau^{t_i-2} \exp(-\delta^{p_i})$$

$I_{\mathrm{Pol}} = 6$ and $I_{\mathrm{Exp}} = 6$ for Eq. (12), $I_{\mathrm{Pol}} = 5$ and $I_{\mathrm{Exp}} = 7$ for Eq. (13)

Results of this formulation were already discussed in the preceding sections, where Eq. (12) was referred to as the "simultaneously optimized equation of state with 12 terms" where nonpolar fluids were discussed. The numerical stability of Eq. (12) and the extrapolation behavior of equations of state based on Eq. (12) were analyzed in Section 3.3. The representation of speeds of sound at liquid states was shown in Fig. 5. Plots of ideal curves were presented in Figs. 9 and 10. The accuracy of predicted isochoric heat capacities was shown in Fig. 11. As a very global quality criterion, Fig. 13 shows weighted variances which resulted from fits of Eq. (12) to the considered data sets and from refitted Bender [18] equations of state. Since the data sets were weighted with the demanded uncertainties summarized in Table I, the weighted variances are a direct measure for the fulfillment of the formulated demands. In general, weighted variances $\sigma^2_{wt} < 0.3$ indicate completely satisfactory results. The new equations of state describe the selected data sets with weighted variances $\sigma^2_{wt} < 0.3$ with only two exceptions, isobutane ($\sigma^2_{wt} = 0.34$) and SF_6 ($\sigma^2_{wt} = 0.38$), which will be discussed in Ref. 15. On average, the weighted variance which results from fitting Eq. (12) to data sets for non- or weakly polar substances is less than half the size of the weighted variance which results from refitted Bender equations with 19 terms.

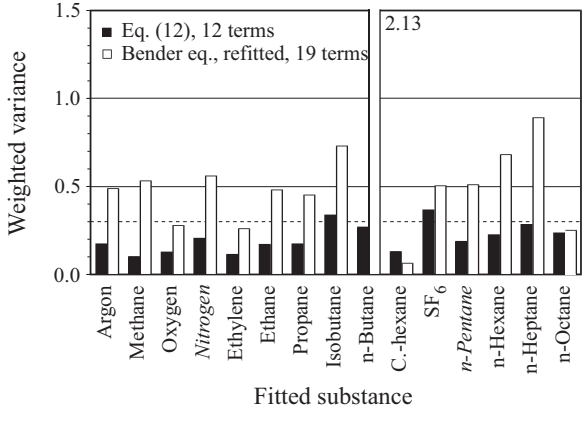

Fig. 13. Weighted variances resulting from fits of equations of state based on the simultaneously optimized functional form for non- and weakly polar fluids, Eq. (12), and of Bender equations [18] to data sets of 15 non- and weakly polar fluids. The data sets for nitrogen and *n*-pentane were not used in the simultaneous optimization.

4.2. Results for Typical Polar Fluids

Data sets for a total of 13 polar substances were considered when working on a simultaneously optimized functional form for these fluids. The critical temperatures of the fluids considered in comparisons and in the optimization procedure covered the range from $T_c = 282.35$ K for ethylene to $T_c = 456.82$ K for 2,2-dichloro-1,1,1-trifluoroethane (HCFC-123) and $T_c = 487.12$ K for 1,1,2-trichlorotrifluoroethane (CFC-113), respectively. The acentric factors covered the range from $\omega \approx 0.087$ for ethylene to $\omega \approx 0.327$ for 1,1,1,2-tetrafluoroethane (HFC-134a). The dipole moments of the fluids cover the range from $\mu = 0$ for carbon dioxide, which is still considered polar due to a qudrupole moment of $Q = 1.5 \cdot 10^{-39}$ C·m^2, to $\mu = 7.74 \cdot 10^{-30}$ C·m for 1,1,1-trifluoroethane (HFC-143a). At low reduced temperatures, experimental data were considered down to the triple point of dichlorodifluoromethane (CFC-12) at $T_t/T_c \approx 0.301$. At high reduced temperatures, data were considered up to the limits which result from the experimental data available for carbon dioxide ($T_{max}/T_c \approx 3.38$), ammonia ($T_{max}/T_c \approx 1.42$), and chlorodifluoromethane (HCFC-22, $T_{max}/T_c \approx 1.42$). Data at pressures above $p_{max} \approx 100$ MPa were not considered.

Based on the selected data sets for the halogenated hydrocarbons dichlorodifluoromethane (CFC-12), chlorodifluoromethane (HCFC-22), difluoromethane (HFC-32), 2,2-dichloro-1,1,1-trifluoroethane (HCFC-123), pentafluoroethane (HFC-125), 1,1,1,2-tetrafluoroethane (HFC-134a), 1,1,1-trifluoroethane (HFC-143a), and 1,1-difluoroethane (HFC-152a) and on data sets for ethylene, carbon dioxide, and ammonia, the simultaneous optimization algorithm resulted in the following functional form for technical equations of state for typical polar fluids:

$$\begin{aligned}\alpha(\tau,\delta) &= \alpha^{o}(\tau,\delta)+\alpha^{r}(\tau,\delta)\\ &= \alpha^{o}(\tau,\delta)+n_1\delta\tau^{0.250} \quad +n_2\delta\tau^{1.250} \quad +n_3\delta\tau^{1.500}\\ &\quad +n_4\delta^3\tau^{0.250} \quad +n_5\delta^7\tau^{0.875} \quad +n_6\delta\tau^{2.375}e^{-\delta}\\ &\quad +n_7\delta^2\tau^{2.000}e^{-\delta}+n_8\delta^5\tau^{2.125}e^{-\delta} \quad +n_9\delta\tau^{3.500}e^{-\delta^2}\\ &\quad +n_{10}\delta\tau^{6.50}e^{-\delta^2}+n_{11}\delta^4\tau^{4.75}e^{-\delta^2}+n_{12}\delta^2\tau^{12.5}e^{-\delta^3}, \qquad (13)\end{aligned}$$

with the reduced Helmholtz energy $\alpha = a/(RT)$, the temperature T, the gas constant R, the inversely reduced temperature $\tau = T_c/T$, and the reduced density $\delta = \rho/\rho_c$. The substance-specific parameters T_c, ρ_c, R, and n_i which are needed to evaluate Eq. (13) and the sources of the correlations used for the ideal gas contribution, $\alpha^{o}(\tau,\delta)$, are given in Ref. 16. The derivatives of Eq. (13) which are needed to calculate common thermodynamic properties are summarized in Table IV. The data sets for trichlorofluoromethane

(CFC-11) and 1,1,2-trichlorotrifluoroethane (CFC-113) were used to test the applicability of Eq. (13) to polar fluids, which were not considered in the simultaneous optimization procedure—again, no significant disadvantages were found for these substances. For ethylene, the equation of state which uses the simultaneously optimized functional form for non- and weakly polar fluids, Eq. (12), yields slightly better results and thus no substance-specific parameters for ethylene are presented in Ref. 16.

Results of an equation of state for 1,1,1,2-tetrafluoroethane (HFC-134a) which is based on the new functional form for polar fluids, Eq. (13), were already shown in Fig. 6. As a very global quality criterion, Fig. 14 shows weighted variances which resulted from fits of Eq. (13) to the considered data sets and from refitted Bender [18] equations of state. In general, the new equations of state describe the available data sets with weighted variances $\sigma^2_{wt} < 0.3$. The only exceptions, dichlorodifluoromethane (CFC-12, $\sigma^2_{wt} = 0.35$), carbon dioxide ($\sigma^2_{wt} = 0.36$), and ammonia ($\sigma^2_{wt} = 0.43$), will be discussed in more detail below and in Ref. 16. On average, the weighted variance which results from fitting Eq. (13) to data sets for polar substances is less than a quarter of the size of the weighted variance which results from refitted Bender equations with 19 terms. To demonstrate the superior extrapolation behavior of the new functional form, Fig. 15 shows ideal curves for 1,1,2-trichlorotrifluoroethane (CFC-113) calculated from the new equation of state and from a refitted Bender equation of state; among the considered polar fluids the data set for 1,1,2-trichlorotrifluoroethane is the most restricted one.

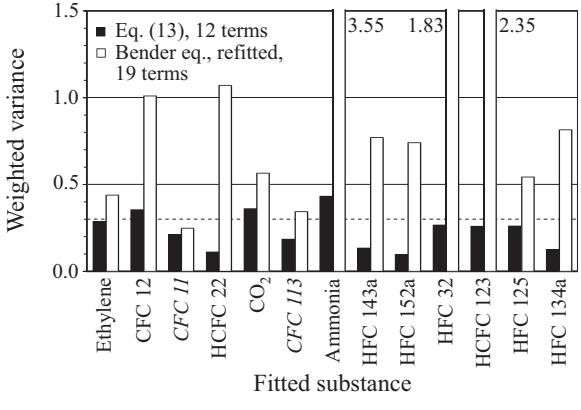

Fig. 14. Weighted variances resulting from fits of equations of state based on the simultaneously optimized functional form for typical polar fluids, Eq. (13), and of Bender equations [18] to data sets of 13 polar fluids. The data sets for the refrigerants CFC-11 and CFC-113 were not used in the simultaneous optimization.

Two limitations have to be considered when setting up equations of state based on the new functional form for polar fluids, Eq. (13). Since most of the considered polar substances are organic compounds for which dissociation becomes relevant at rather low reduced temperatures, the data sets used to develop Eq. (13) were restricted in the limit of high reduced temperatures. For carbon dioxide, data were available up to $T_{max}/T_c \approx 3.38$ but no data were available at $T/T_c > 1.42$ for any of the other substances. Based only on data for carbon dioxide, it was therefore not possible to describe the range of high reduced temperatures as accurately as for non- and weakly polar fluids. For carbon dioxide, enlarged uncertainties are observed at temperatures above $T/T_c \approx 1.5$ (for details see Ref. 16), even though the high temperature range is qualitatively correctly described by equations of state based on the new functional form; see Fig. 15. Any attempt to improve the representation of carbon dioxide data at high temperatures affected the representation of the data sets for other fluids. Thus it was accepted that increased uncertainties are to be expected when using equations of state based on Eq. (13) at high reduced temperatures.

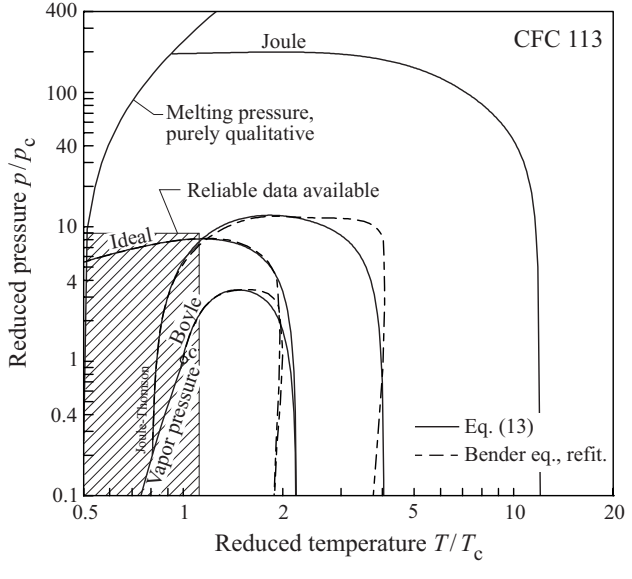

Fig. 15. Ideal curves of 1,1,2-trichlorotrifluoroethane (CFC-113) calculated from the equation of state based on the new functional form for polar fluids, Eq. (13), and from a refitted Bender [18] equation of state. In a reasonable range of pressures and temperatures, no Joule-inversion is predicted by the Bender equation. The hatched area corresponds to the region where reliable data were available to fit the equations.

Weakly associating fluids can be described rather well with equations of state based on the new functional form for polar fluids. Even the equation of state for ammonia satisfies the demands formulated in Table I with just a few exceptions; see Ref. 16. However, strongly associating fluids cannot be described with the demanded accuracy; a corresponding attempt for water failed. Thus, when dealing with associating fluids, functional forms according to Eq. (13) should be used with special care. An application of the new concept to strongly associating fluids is one of the tasks which is still pending. Whether associating fluids can simply be treated as a further group of fluids or whether an extension has to rely on different approaches in this case is not yet clear.

5. PROSPECTS

Based on the simultaneously optimized functional forms presented above, state-of-the-art technical equations of state have been developed for 27 fluids. The results for non- and weakly polar fluids are summarized in detail in Ref. 15, those for polar fluids in Ref. 16. Equations of state for other fluids belonging to the same groups are being developed and will be published in further articles of this series. However, up to now we have mainly been replacing obsolete technical equations of state by more accurate and more reliable equations—multiparameter equations of state were available for all of the fluids discussed here. The brief discussion of the status quo in Section 2 shows that this first step is certainly valuable in itself, but the aim of this project is to proceed to fluids which have not been described with multiparameter equations before. To do so implies a number of challenges of both a theoretical and experimental nature.

Limitations of the functional forms proposed here have to be investigated in more detail. In Section 4.2 problems with regard to the representation of strongly associating fluids have been discussed. It has not yet been investigated systematically whether restrictions apply for other groups of substances like, e.g., aromatic compounds. Thus, it might become necessary to develop simultaneously optimized functional forms for further groups of substances where only restricted data sets are available. In this case, additional experimental work would be necessary to establish reference data sets for selected fluids out of the corresponding groups, which can be used in the simultaneous optimization process. Once a suitable functional form is established, rather small data sets are sufficient to describe other fluids out of the same group; see Section 5.1.

In this sense, small but reliable data sets of appropriate accuracy are required to establish further equations of state based on the functional forms presented in this article. Available pure component databases contain

data for a multitude of fluids. However, the accuracy of these data is questionable and difficult to assess in many cases. Undetected systematic errors in the used data sets are likely to affect the performance of equations of state based on existing databases. Algorithms which automatically detect inconsistencies in data sets resulting from such systematic experimental errors need to be developed. However, measurements with experimental equipment optimized for the data needs of technical equations of state could be the more favorable way to proceed if accuracy is essential. Demands on data sets taken either from published sources or from these measurements are discussed in the following section. In order to enable other scientists to contribute to this project, software for fitting equations of state based on simultaneously optimized functional forms to their own data can be made available.

5.1. Requirements on the Data Sets

As mentioned above, two very different situations exist when discussing requirements on the data set which is necessary to establish a technical equation of state by fitting the coefficients of a given simultaneously optimized functional form.

When equations are based solely on data published in the scientific literature, there is little chance to exercise any influence on the number of available data, on the properties which have been measured, or on the distribution of the data. Surprisingly small data sets with a very unbalanced distribution of the data proved to be sufficient to establish equations of state which yield reliable results even far outside of the region where data were available. However, this has to be verified in every single case. Absolute plots of derived caloric properties (see Fig. 3) or plots of ideal curves (see Figs. 9, 10, and 15 and Ref. 34) calculated from the resulting equation are sensitive tools to detect unreasonable behavior. Equations which were not fitted at least to vapor pressures and to data for thermal properties at liquid states cannot be expected to describe the whole range of fluid states. Critical parameters may be obtained from predictive algorithms with sufficient accuracy; see Section 3.3.2. An equation for the heat capacity of the ideal gas is required to describe caloric properties; for the integration which is necessary to obtain $\alpha^{\circ}(\tau, \delta)$, see Ref. 13.

In many cases, additional measurements will become necessary to verify data from the literature, to supplement published data, or as the only source of experimental information. At this point it becomes much more important to discuss requirements on the available data sets. The assessment summarized in the following paragraphs is based on experience gained during the development of the equations of state presented in this

article and in Refs. 15 and 16 and on investigations with systematically reduced data sets; see for example Section 3.3.1.

For substances with simple molecular structure, the required information on caloric properties of the ideal gas can usually be derived from published spectroscopic data with sufficiently high accuracy. Where such information is not available, where the molecular structure becomes too complicated, or where features like hindered internal rotations make an accurate theoretically founded prediction of ideal gas heat capacities difficult, gas phase speeds of sound measured with spherical resonators are the most reliable source of information on caloric properties of the ideal gas. In this case, such data are needed over a range of temperatures which is as broad as possible, but 10–20 data points are usually sufficient, since the temperature dependence of the ideal gas heat capacity is easy to fit.

At reduced temperatures below $T/T_c \approx 0.9$, information which constrains the second virial coefficients calculated from the equation of state is sufficient to guarantee the required accuracy in the gas phase. This information can also be obtained most easily from speed of sound measurements with spherical resonators. Usually about three isotherms with five data points each will be sufficient to enable an accurate representation of gas phase properties. However, since the residual contribution to the speed of sound is very small in the gas phase, the speeds of sound need to be fitted to far less than the demanded uncertainty of $|\Delta w|/w = 1\%$ to guarantee a sufficiently accurate description of $p\rho T$ data. When the resulting equation does not represent gas phase speeds of sound clearly within $|\Delta w|/w < 0.1\%$ for pressures below about 1 MPa the second acoustic virial coefficient should be checked to ensure that it is represented within $|\Delta\beta_a|/\beta_a \leqslant \approx 2\%$. Larger deviations in β_a and B are common at $T/T_c < \approx 0.7$ where the plot of the second virial coefficients becomes very steep.

For liquid and supercritical states, it is most advantageous to rely on measured $p\rho T$ data. The data set does not need to be large—about 30–50 data points should be sufficient (results were discussed in Section 3.3.1 which were obtained with an even smaller data set), but the data should cover a sufficiently broad range of states and they should be clearly more accurate than the resulting equation needs to be. Significant systematic errors in parts of the data set are likely to distort the prediction of derived properties. To enable the resulting equation to fulfill the demands on accuracy summarized in Table I, an experimental uncertainty of $|\Delta\rho|/\rho \leqslant 0.05\%$ should be aimed for at $p \leqslant 30$ MPa; at $p > 30$ MPa uncertainties of $|\Delta\rho|/\rho \leqslant 0.1\%$–$0.2\%$ can be regarded as sufficient.

Information on thermal properties at phase equilibrium is essential to describe the phase equilibrium itself and to achieve a consistent description

of caloric properties in the liquid phase. However, since the temperature dependence of these properties is predicted rather accurately by equations with a simultaneously optimized functional form, data sets with 5–10 accurate vapor pressures and saturated liquid densities should be sufficient. If possible, the data should cover the range $T_t \leqslant T \leqslant \approx 0.99T_c$. A set of 3–5 data for the saturated vapor density is helpful mainly at temperatures in the range $\approx 0.9T_c \leqslant T \leqslant \approx 0.99T_c$. At temperatures in the range $\approx 0.99T_c < T < T_c$, vapor pressures can still be represented accurately, but the uncertainty of calculated values for the saturated vapor and liquid density increases due to fundamental restrictions of simple technical equations of state. If such data are used in fits with high weights, they may affect the representation of properties in other regions. At low reduced temperatures, the relative uncertainty of results on the vapor pressure increases due to experimental difficulties regarding the measurement of small pressures and due to an increasing influence of impurities. If such data are overfitted, they may distort the representation of other properties as well. When an accurate description of vapor pressures at low reduced temperatures is regarded as important, it may be useful to include some data for the enthalpy of evaporation, Δh_v, at these conditions.

Some data on derived caloric properties such as the isochoric heat capacity or the speed of sound at liquid and liquid-like supercritical states are helpful to verify a certain level of accuracy for these properties. But in general, reasonable predictions can be expected if the equation was fitted to a consistent set of thermal properties. Increased uncertainties may be encountered at low reduced temperatures.

The requirements on data sets discussed above may seem excessive and difficult to fulfill. However, problems result only from the broad range of states and from the fact that different properties should be covered ideally. The total number of data points which is needed to establish an equation of state of the new class is on the order of 100 and can be measured rapidly if suitable experimental equipment are available. Compared to other multiparameter equations of state which are usually based on hundreds or even thousands of data points, this is a substantial advantage.

ACKNOWLEDGMENTS

The authors are indebted to the Deutsche Forschungsgemeinschaft for their financial support and to Prof. R. T Jacobsen and Dr. E. W. Lemmon, whose literature database *BIBLIO* was very helpful for setting up the required data sets.

REFERENCES

1. U. Setzmann and W. Wagner, *J. Phys. Chem. Ref. Data* **20**:1061 (1991).
2. R. Span and W. Wagner, *J. Phys. Chem. Ref. Data* **25**:1509 (1996).
3. W. Wagner and A. Pruß, *J. Phys. Chem. Ref. Data* **31**:387 (2002).
4. C. Tegeler, R. Span, and W. Wagner, *J. Phys. Chem. Ref. Data* **28**:779 (1999).
5. R. Span, E. W. Lemmon, R. T Jacobsen, W. Wagner, and A. Yokozeki, *J. Phys. Chem. Ref. Data* **29**:1361 (2000).
6. J. Smukala, R. Span, and W. Wagner, *J. Phys. Chem. Ref. Data* **29**:1053 (2000).
7. R. Schmidt and W. Wagner, *Fluid Phase Equil.* **19**:175 (1985).
8. R. S. Katti, R. T Jacobsen, R. B. Stewart, and M. Jahangiri, *Adv. Cryo. Eng.* **31**:1189 (1986).
9. K. M. de Reuck and R. J. B. Craven, *International Thermodynamic Tables of the Fluid State—12. Methanol* (Blackwell Scientific, London, 1993).
10. R. Tillner-Roth and H. D. Baehr, *J. Phys. Chem. Ref. Data* **23**:657 (1994).
11. R. Tillner-Roth and A. Yokozeki, *J. Phys. Chem. Ref. Data* **26**:1273 (1997).
12. E. W. Lemmon, R. T Jacobsen, S. G. Penoncello, and D. G. Friend, *J. Phys. Chem. Ref. Data* **29**:331 (2000).
13. R. Span, *Multiparameter Equations of State—An Accurate Source of Thermodynamic Property Data* (Springer, Berlin, 2000).
14. R. Span, H.-J. Collmann, and W. Wagner, *Int. J. Thermophys.* **19**:491 (1998).
15. R. Span and W. Wagner, *Int. J. Thermophys.* **24**:41 (2003).
16. R. Span and W. Wagner, *Int. J. Thermophys.* **24**:111 (2003).
17. M. Benedict, G. B. Webb, and L. C. Rubin, *J. Chem. Physics* **8**:334 (1940).
18. E. Bender, Equations of state exactly representing the phase behavior of pure substances, in *Proc. 5th Symp. Thermophys. Prop.* (ASME, New York, 1970), pp. 227–235.
19. R. T Jacobsen and R. B. Stewart, *J. Phys. Chem. Ref. Data* **2**:757 (1973).
20. W. Duschek, R. Kleinrahm, and W. Wagner, *J. Chem. Thermodynamics* **22**:827 (1990).
21. R. Gilgen, R. Kleinrahm, and W. Wagner, *J. Chem. Thermodynamics* **24**:1243 (1992).
22. K. Brachthäuser, R. Kleinrahm, H.-W. Lösch, and W. Wagner, *VDI-Fortschritt Ber.,* Reihe 8, No. 371 (VDI-Verlag, Düsseldorf, 1993).
23. J. Klimeck, R. Kleinrahm, and W. Wagner, *J. Chem. Thermodynamics* **33**:251 (2001); (a) P. H. Salim and M. A. Trebble, *Fluid Phase Equil.* **65**:41 (1991).
24. R. Niepmann, *J. Chem. Thermodynamics* **16**:851 (1984).
25. A. Polt, *Zur Beschreibung Thermodynamischer Eigenschaften reiner Fluide mit "Erweiterten BWR-Gleichungen,"* Ph.D. thesis (University Kaiserslautern, 1987).
26. E. W. Lemmon and R. Tillner-Roth, *Fluid Phase Equil.* **165**:1 (1999).
27. J. Ahrendts and H. D. Baehr, *Int. J. Chem. Eng.* **21**:557 (1981).
28. J. Ahrendts and H. D. Baehr, *Int. J. Chem. Eng.* **21**:572 (1981).
29. U. Setzmann and W. Wagner, *Int. J. Thermophys.* **10**:1103 (1989).
30. R. T Jacobsen, S. G. Penoncello, E. W. Lemmon, and R. Span, Multiparameter equations of state, in *Equations of State for Fluids and Fluid Mixtures*, J. V. Sengers, R. F. Kayser, C. J. Peters, and H. J. White Jr., eds. (Elsevier, Amsterdam, 2000).
31. B. Saager, R. Hennenberg, and J. Fischer, *Fluid Phase Equil.* **72**:41 (1992).
32. C. Tegeler, R. Span, and W. Wagner, *VDI Fortschritt-Berichte,* Reihe 3, No. 480 (VDI-Verlag, Düsseldorf, 1997).
33. E. A. Mason and T. H. Spurling, The virial equation of state, in *The International Encyclopedia of Physical Chemistry and Chemical Physics* (Pergamon, Oxford, 1969).
34. R. Span and W. Wagner, *Int. J. Thermophys.* **18**:1415 (1997).
35. A. S. Teja, R. J. Lee, D. Rosenthal, and M. Anselme, *Fluid Phase Equil.* **56**:153 (1990).

36. L. Riedel, *Chem. Eng. Tech.* **35**:433 (1963).
37. G. R. Somayajulu, *J. Chem. Eng. Data* **34**:106 (1989).
38. A. Vetere, *Fluid Phase Equil.* **109**:17 (1995).
39. R. Tillner-Roth and H. D. Baehr, *J. Chem. Thermodynamics* **24**:413 (1992).
40. R. Tillner-Roth and H. D. Baehr, *J. Chem. Thermodynamics* **25**:277 (1993).
41. M. Dressner and K. Bier, *VDI Fortschritt-Berichte,* Reihe 3, No. 332 (VDI-Verlag, Düsseldorf, 1993).
42. J. Klomfar, J. Hruby, and O. Šifner, *Int. J. Thermophys.* **14**:727 (1993).
43. I. M. Abdulagatov, *Experimental Results for the Isochoric Heat Capacity of n-Heptane and n-Octane*. Private communication (National Institute of Standards and Technology, Boulder, Colorado, 1998).